Hermite–Gaussian breathers and solitons in strongly nonlocal nonlinear media

Dongmei Deng, Xin Zhao, Qi Guo,* and Sheng Lan

Laboratory of Photonic Information Technology, South China Normal University, Guangzhou 510631, China
**Corresponding author: dmdeng@263.net*

Received April 5, 2007; revised June 21, 2007; accepted July 13, 2007;
posted July 17, 2007 (Doc. ID 81860); published August 31, 2007

Based on the Snyder–Mitchell model in the Cartesian coordinate system, exact analytical Hermite–Gaussian (HG) solutions are obtained in strongly nonlocal nonlinear media. The comparisons of analytical solutions with numerical simulations of the nonlocal nonlinear Schrödinger equation show that the analytical HG solutions are in good agreement with the numerical simulations in the case of strong nonlocality. Furthermore, we demonstrate that HG functions can be expressed as a linear superposition of individual Gaussian functions with a π phase difference under the appropriate conditions. © 2007 Optical Society of America

OCIS codes: 190.5530, 190.4360, 060.1810.

1. INTRODUCTION

As is well known, optical spatial solitons in nonlocal nonlinear media have received much attention lately [1–30] due to their rich potential applications to photonic switching [1], all-optical switching and logic gating [2], and all-optical signal processing [3]. Optical spatial solitons are self-trapped optical beams that exist by virtue of the balance between diffraction and nonlinearity. When the balance between diffraction and nonlinearity is broken, optical beams become breathers. The propagation of the optical beams in the nonlocal nonlinear media is modeled by the nonlocal nonlinear Schrödinger equation (NNLSE) [1,4,5]. Snyder and Mitchell [1] simplified the NNLSE to a linear model named the Snyder–Mitchell model [31] in the strongly nonlocal case, and they found an exact Gaussian-shaped stationary solution called an accessible soliton. Subsequently, Assanto's team observed accessible solitons in nematic liquid crystal (NLC) [6,7], called nematicons [3], and they proved theoretically [6] and experimentally [7] that NLC is one of the strongly nonlocal nonlinear materials. Recently, Guo's group found a new approximate model for the NNLSE in strongly nonlocal nonlinear media (SNNM) with a symmetrical real spatial response function by using the Taylor expansion method; they obtained the exact solution of Gaussian breathers and a large phase shift of the Gaussian soliton comparable with its local counterpart [8–10].

In local nonlinear media, the complex-form solitons cannot be self-guided because of the natural repulsion existing between lobes of opposite phase. In nonlocal nonlinear media, nonlocality makes it possible to overcome repulsion between out-of-phase bright [11–16,32] or in-phase dark solitons [17] that can form bound complex states observed in one-dimensional settings [13,18]. McLaughlin *et al.* predicted that NLC can sustain higher-order mode solitons, and they obtained several higher-order mode solutions by numerical simulation [19]. Then, Hutsebaut *et al.* demonstrated experimentally that the higher-order mode solitons traveled stably in NLC [13]. The stability of multipole-mode solitons in nonlocal nonlinear media was addressed by Xu *et al.* [14]. Rotschild *et al.* [20] presented the experimental observation of scalar multipole solitons in SNNM. Laguerre and Hermite soliton clusters in nonlocal nonlinear media have been introduced by Buccoliero *et al.* [21]. However, to the best of our knowledge, exact analytical solutions with the Hermite–Gaussian (HG) form have remained unexplored in SNNM. Hence it is necessary to derive the exact analytical solutions with the HG form in SNNM. Our purpose in this paper is to introduce HG solutions and to study their propagation properties in SNNM.

The paper is organized as follows. First, based on the Snyder–Mitchell linear model in the rectangular coordinate system, we obtain the exact $(1+D)$-dimensional ($D=1,2$) analytical solutions with the HG form in the SNNM. Second, we discuss the solutions, the comparisons of analytical solutions with numerical simulations of the NNLSE are given, and we find that any order HG function can be expressed as a linear superposition of individual Gaussian functions with a π phase difference under the appropriate conditions. HG solitons can be thought as a bound state of individual Gaussian solitons. Finally, a conclusion is presented.

2. (1+1)-DIMENSIONAL HG BREATHERS AND SOLITONS OF THE SNYDER–MITCHELL MODEL

The propagation of the optical beams in the $(1+D)$-dimensional ($D=1,2$) nonlocal cubic nonlinear media is governed by the NNLSE [1,4,5]:

$$i\frac{\partial\varphi}{\partial z}+\mu\Delta_{\perp}\varphi+k\eta\varphi\int R(\mathbf{x}-\mathbf{x}')|\varphi(\mathbf{x}',z)|^2\mathrm{d}^D\mathbf{x}'=0, \quad (1)$$

where $\varphi=\varphi(\mathbf{x},z)$ is a paraxial beam, z is the longitudinal coordinate, $\mu=1/2k$, $k=\omega n_0/c$ is the wave number in the

media without nonlinearity, η is a material constant ($\eta>0$ or $\eta<0$ corresponds to a focusing or defocusing material), $\mathbf{x}$ and $\mathbf{x}'$ are the D-dimensional transverse coordinate vectors, $\Delta_\perp$ is the D-dimensional transverse Laplacian operator, and R is the normalized symmetrical real spatial response function of the media.

For the strongly nonlocal case, the NNLSE can be deduced as the Snyder–Mitchell linear model [1,9,10]:

$$i\frac{\partial\varphi}{\partial z}+\mu\Delta_\perp\varphi-\frac{1}{2}k\eta\gamma P_0 r^2\varphi=0, \tag{2}$$

where $\gamma(>0)$ is the material parameter associated with the response function R, $r=|\mathbf{x}|$ is the transverse distance from the beam center in the coordinate system, and $P_0=\int_{-\infty}^{\infty}|\varphi(\mathbf{x},0)|^2 d^D\mathbf{x}$ is the input power of the beam at $z=0$.

For the (1+1)-dimensional case, Eq. (2) can be reduced to

$$i\frac{\partial\varphi}{\partial z}+\mu\frac{\partial^2\varphi}{\partial x^2}-\frac{1}{2}k\eta\gamma P_0 x^2\varphi=0. \tag{3}$$

We search for a solution to Eq. (3) by writing it as a multiplication of the two functions $F(x,z)$ and $\varphi_G(x,z)$,

$$\varphi=F(x,z)\varphi_G(x,z). \tag{4}$$

Substituting Eq. (4) into Eq. (3), we obtain

$$i\frac{\partial F}{\partial z}\varphi_G+\mu\frac{\partial^2 F}{\partial x^2}\varphi_G+2\mu\frac{\partial F}{\partial x}\frac{\partial\varphi_G}{\partial x}+F\left(i\frac{\partial\varphi_G}{\partial z}+\mu\frac{\partial^2\varphi_G}{\partial x^2}-\frac{1}{2}k\eta\gamma P_0 x^2\varphi_G\right)=0. \tag{5}$$

If we suppose

$$i\frac{\partial\varphi_G}{\partial z}+\mu\frac{\partial^2\varphi_G}{\partial x^2}-\frac{1}{2}k\eta\gamma P_0 x^2\varphi_G=0, \tag{6}$$

then we can obtain from Eq. (5) simultaneously that

$$i\frac{\partial F}{\partial z}\varphi_G+\mu\frac{\partial^2 F}{\partial x^2}\varphi_G+2\mu\frac{\partial F}{\partial x}\frac{\partial\varphi_G}{\partial x}=0. \tag{7}$$

It is known [1,9] that the solution of Eq. (6) is the Gaussian function

$$\varphi_G=\frac{\sqrt{P_0}\exp[i\theta(z)]}{[\sqrt{\pi}w(z)]^{1/2}}\exp\left[-\frac{x^2}{2w(z)^2}+ic(z)x^2\right], \tag{8}$$

where $w(z)$ is the beam width of the Gaussian beam, $c(z)$ represents the phase-front curvature of the beam, and $\theta(z)$ is the phase of the complex amplitude. They are given by [9], respectively,

$$w(z)^2=w_0^2\left(\frac{P_c}{P_0}\sin^2\beta_0 z+\cos^2\beta_0 z\right), \tag{9}$$

$$c(z)=\frac{k\beta_0\left(\frac{P_c}{P_0}-1\right)\sin 2\beta_0 z}{4\left(\cos^2\beta_0 z+\frac{P_c}{P_0}\sin^2\beta_0 z\right)}, \tag{10}$$

$$\theta(z)=-\frac{1}{2}\arctan\left(\sqrt{\frac{P_c}{P_0}}\tan\beta_0 z\right), \tag{11}$$

$$P_c=\frac{1}{k^2\gamma\eta w_0^4}, \tag{12}$$

where w_0 is the initial beam width of the Gaussian beam at $z=0$, $\beta_0=\sqrt{\eta\gamma P_0}$, and P_c is the critical power for soliton propagation. Equation (9) shows that the z-dependent function $w(z)$, which is the beam width of the Gaussian function obtained by Snyder and Mitchell [1], oscillates periodically along the propagation z if $P_0\neq P_c$. If we divide w_0^2 into both sides of Eq. (9), Eq. (9) becomes Eq. (4) obtained by Snyder and Mitchell [1].

Substituting Eq. (8) into Eq. (7) yields

$$i\frac{\partial F}{\partial z}+\mu\frac{\partial^2 F}{\partial x^2}+\left(4i\mu c-\frac{2\mu}{w(z)^2}\right)x\frac{\partial F}{\partial x}=0. \tag{13}$$

Making the variable transform

$$\xi=\frac{x}{w(z)},\qquad \zeta=z \tag{14}$$

and using Eqs. (9) and (10), we can reduce Eq. (13) to

$$\frac{\partial^2 F}{\partial\xi^2}-2\xi\frac{\partial F}{\partial\xi}+2ikw(\zeta)^2\frac{\partial F}{\partial\zeta}=0. \tag{15}$$

By use of the method of separation of variables, letting $F=X(\xi)\Theta(\zeta)$, Eq. (15) is separated into the following two differential equations:

$$\frac{d^2X}{d\xi^2}-2\xi\frac{dX}{d\xi}+2nX=0, \tag{16}$$

$$\frac{d\Theta}{d\zeta}+\frac{in}{kw(\zeta)^2}\Theta=0, \tag{17}$$

where n is an integer; Eq. (16) is the well-known Hermite differential equation [33]. From Eqs. (16) and (17), we can derive

$$X=H_n(\xi)=H_n\left(\frac{x}{w(z)}\right), \tag{18}$$

$$\Theta=\exp\left[-in\arctan\left(\sqrt{\frac{P_c}{P_0}}\tan\beta_0 z\right)\right]. \tag{19}$$

Then by substitution of Eqs. (8), (18), and (19) into Eq. (4), the exact solutions of Eq. (3) can be obtained,

$$\varphi_n=\frac{C_n}{\sqrt{w(z)}}H_n\left(\frac{x}{w(z)}\right)\exp\left[-\frac{x^2}{2w(z)^2}\right]\exp\{i[c(z)x^2+(2n+1)\theta(z)]\}, \tag{20}$$

where $C_n=[P_0/(\sqrt{\pi}2^n n!)]^{1/2}$ is the normalized coefficient, $w(z)$, $c(z)$, $\theta(z)$, and P_c are given by Eqs. (9)–(12). When $n=0$, Eq. (20) is simplified to the zeroth-order HG solution, i.e., the Gaussian solution,

$$\varphi_0 = \frac{\sqrt{P_0}}{[\sqrt{\pi}w(z)]^{1/2}} \exp\left[-\frac{x^2}{2w(z)^2}\right] \exp\{i[c(z)x^2 + \theta(z)]\}. \tag{21}$$

Equation (21) is the Gaussian solution obtained by Snyder and Mitchell for the (1+1)-dimensional case [1].

3. DISCUSSION OF SOLUTIONS

The HG-shaped solutions are the exact solutions to Eq. (2), but the approximate ones to Eq. (1). Comparing Eq. (21) with Eq. (20), we find that the phase-front curvature of the HG beam $c(z)$ is exactly the same as that of the Gaussian beam. The phase $\theta(z)$ is the same as that of the Gaussian solution, except for an additional phase $2n\,\theta(z)$.

A. Comparison with Numerical Simulation of the NNLSE

Figures 1–3 show the comparison of the exact analytical solutions for the Snyder–Mitchell model in the Cartesian coordinate system with the exact results of a numerical simulation of Eq. (1). It can be found from Figs. 1–3 that the analytical solutions are in good agreement with the numerical simulations.

To simulate the propagation, we use the input HG beam parameters, i.e., $\varphi_n(x,0)=(C_n/\sqrt{w_0})H_n(x/w_0)\times\exp(-x^2/2w_0^2)$, and assume that the material response is the Gaussian function [4,5,8], i.e., $R(x)=(1/\sqrt{2\pi}w_m)\times\exp(-x^2/2w_m^2)$, where w_m is the characteristic length of the material response function, $\alpha=w_{0n}/w_m$ denotes the degree of the material nonlocality; for numerical simulations, $w_{0n}=\sqrt{2n+1}w_0$, which is the initial HG beam width, can be obtained by using the definition of the second-order moment for beam width. The less α is, the stronger the nonlocality is. Obviously, for a fixed characteristic length of the material response function, α increases with the increased mode number n of the HG beam, and the degree of the nonlocality becomes weak. The normalized variables are given by $Z=z/w_0^2k$, $X=x/w_0$, and $\Phi=kw_0\eta^{1/2}\varphi$. In this paper, the material response function

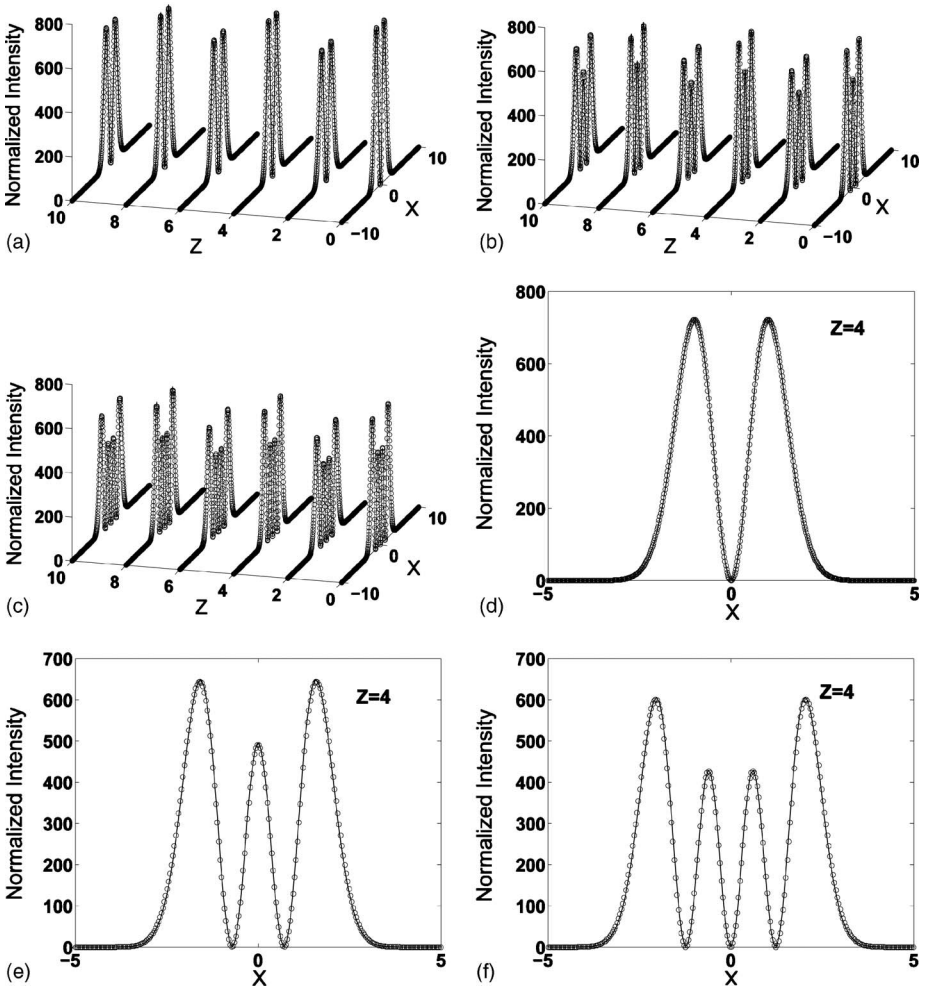

Fig. 1. Evolution of the normalized intensity profiles for (1+1)-dimensional (a) first-, (b) second-, and (c) third-order-mode HG breathers in the Gaussian-shaped response material. Solid curves, numerical simulation; open circles, analytical solution. Solid curves and open circles in (d), (e), and (f) are the normalized intensity distributions at $Z=4$ corresponding to (a), (b), and (c), respectively. The parameters are chosen as $P_0/P_c=0.7$, $\alpha=0.1$.

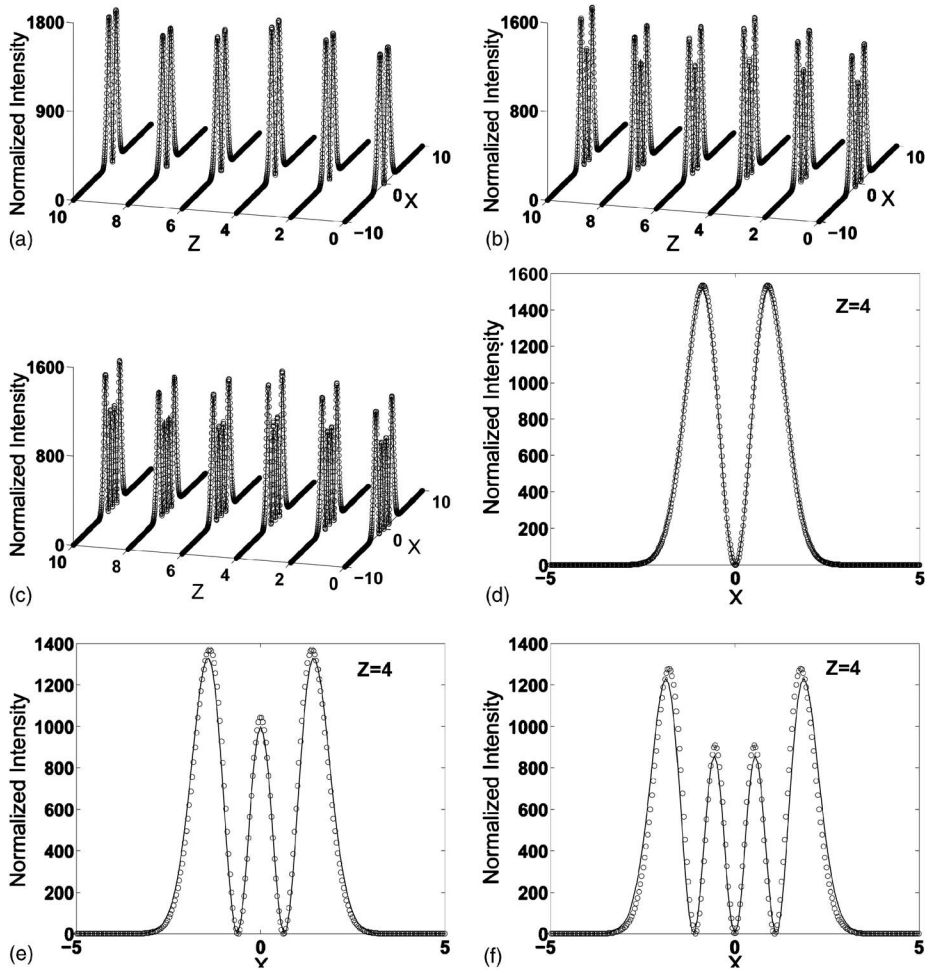

Fig. 2. Evolution of the normalized intensity profiles for (1+1)-dimensional (a) first-, (b) second-, and (c) third-order-mode HG breathers in the Gaussian-shaped response material. Solid curves, numerical simulation; open circles, analytical solution. Solid curves and open circles in (d), (e), and (f) are the normalized intensity distributions at $Z=4$ corresponding to (a), (b), and (c), respectively. The parameters are chosen as $P_0/P_c=1.3$, $\alpha=0.1$.

and the normalized variables are the same, and $\alpha=0.1$ for all figures.

B. HG Breathers

When $P_0<P_c$, beam diffraction initially overcomes beam-induced refraction, and the beam initially expands, whereas the reverse happens and the beam initially contracts when $P_0>P_c$, as shown in Figs. 1 and 2. These are HG breathers whose widths vibrate periodically as they travel in the straight path along the z axis.

When $m=0$, Eq. (20) is simplified to the zeroth-order HG (Gaussian) breather expression, Eq. (21).

The first-, second- and third-order HG breathers are expressed as, respectively,

$$\varphi_1=\frac{\sqrt{P_0}}{[2\sqrt{\pi}w(z)]^{1/2}}\frac{2x}{w(z)}\exp\left[-\frac{x^2}{2w(z)^2}\right]\exp\{i[c(z)x^2+3\theta(z)]\}, \tag{22}$$

$$\varphi_2=\frac{\sqrt{P_0}}{[8\sqrt{\pi}w(z)]^{1/2}}\left\{4\left[\frac{x}{w(z)}\right]^2-2\right\}\exp\left[-\frac{x^2}{2w(z)^2}\right]\times\exp\{i[c(z)x^2+5\theta(z)]\}, \tag{23}$$

$$\varphi_3=\frac{\sqrt{P_0}}{[48\sqrt{\pi}w(z)]^{1/2}}\left\{8\left[\frac{x}{w(z)}\right]^3-12\left[\frac{x}{w(z)}\right]\right\}\times\exp\left[-\frac{x^2}{2w(z)^2}\right]\exp\{i[c(z)x^2+7\theta(z)]\}. \tag{24}$$

Comparing Eqs. (22)–(24) with Eq. (21), it is easy to see that the phase-front curvature of the higher-order HG breathers $c(z)$ is the same as that of Gaussian breather; the phase of HG breathers increases with increasing mode number n. Figures 1 and 2 show that the differences between the analytical solutions and the numerical simulations increase with increased mode number n when the input power P_0 and the degree of the material nonlocality α are the same.

C. HG Solitons

When $P_0=P_c$, diffraction is exactly balanced by nonlinearity, and these are HG solitons that preserve their widths as they travel in the straight path along the z axis. As $P_0=P_c$, Eq. (20) is simplified to an expression of HG solitons,

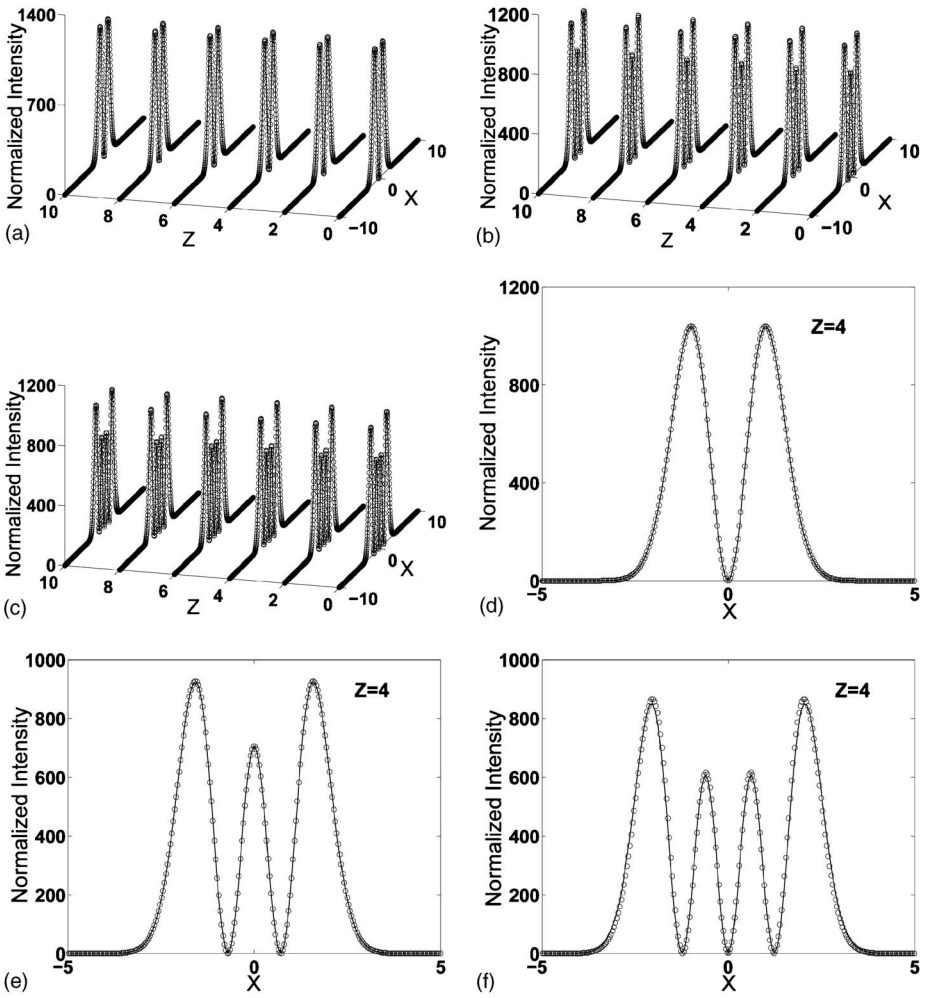

Fig. 3. Stationary propagation of (1+1)-dimensional (a) first-, (b) second-, and (c) third-order-mode HG solitons in the Gaussian-shaped response material up to a distance of $Z=10$. Solid curves, numerical simulation; open circles, analytical solution. Solid curves and open circles in (d), (e), and (f) are the normalized intensity distributions at $Z=4$ corresponding to (a), (b), and (c), respectively. The parameters are chosen as $P_0/P_c=1$, $\alpha=0.1$.

$$\varphi_n = C_n \frac{1}{\sqrt{w_0}} H_n\left(\frac{x}{w_0}\right)\exp\left(-\frac{x^2}{2w_0^2}\right)\exp(-i\beta_n z), \quad (25)$$

where the propagation constant β_n is given by

$$\beta_n = \left(n+\frac{1}{2}\right)\beta_0 = \left(n+\frac{1}{2}\right)\sqrt{\eta\gamma P_0}. \quad (26)$$

Eq. (25) is identical to Eq. (16) of [28], which is written in Chinese. Equation (27) shows that the propagation constant β_n increases as the mode number n increases.

When $n=0$, Eq. (25) is reduced to the zeroth-order HG (Gaussian) soliton expression

$$\varphi_0 = \frac{\sqrt{P_0}}{(\sqrt{\pi}w_0)^{1/2}}\exp\left(-\frac{x^2}{2w_0^2}\right)\exp(-i\beta_0 z). \quad (27)$$

It is evident from Fig. 3 that these different-order-mode HG beams remain invariant as a function of distance z. As expected, our numerical simulations are in excellent agreement with our analytical solutions. If we normalized the intensity by the maximum value of the initial intensity, Figs. 3(d) and 3(e) are consistent with Fig. 7(b) of [19], and Fig. 7(a) in [19] is the well-known Gaussian (the zeroth-order HG) soliton, which demonstrates that waveguide modes shown in [19] are exactly the several low-order-mode HG solitons obtained in our paper. It is indirectly proved that NLC is one of the strong nonlocal nonlinear media.

D. Expression of Higher-Order HG Function by Linear Superposition of Individual Gaussian Functions with π-Phase Difference

The linear superposition of two out-of-phase Gaussian functions can be expressed as

$$\varphi_{01}(x) = A_1\left\{\exp\left[-\frac{(x-a_1)^2}{2}\right]-\exp\left[-\frac{(x+a_1)^2}{2}\right]\right\}$$
$$= A_1\exp\left(-\frac{x^2+a_1^2}{2}\right)[\exp(a_1x)-\exp(-a_1x)]. \quad (28)$$

The first-order HG function can be written as

$$\varphi_1(x) = 2x\exp(-x^2/2). \quad (29)$$

Taylor expanding $[\exp(a_1x)-\exp(-a_1x)]$ with respect to x' at $x'=0$ in Eq. (28), one can obtain

$$\varphi_{01}(x)=A_1\exp\left(-\frac{x^2+a_1^2}{2}\right)\left[2a_1x+\frac{1}{3}a_1^3x^3+\cdots\right]. \tag{30}$$

If the conditions $|a_1x|<1$ and $A_1a_1\exp(-a_1^2/2)=1$ are satisfied, Eq. (30) approaches to Eq. (29) step by step with the decrease of the parameter $|a_1x|$.

The linear superposition of two in-phase functions and one out-of-phase Gaussian function can be expressed as

$$\varphi_{02}(x)=A_2\left\{\exp\left[-\frac{(x-a_2)^2}{2}\right]+\exp\left[-\frac{(x+a_2)^2}{2}\right]\right\}-B_2\exp\left(-\frac{x^2}{2}\right)=A_2\exp\left(-\frac{x^2+a_2^2}{2}\right)[\exp(a_2x)+\exp(-a_2x)]-B_2\exp\left(-\frac{x^2}{2}\right). \tag{31}$$

The second-order HG function can be written as

$$\varphi_2(x)=(4x^2-2)\exp(-x^2/2). \tag{32}$$

Taylor expanding $[\exp(a_2x)+\exp(-a_2x)]$ with respect to x' at $x'=0$ in Eq. (31) yields

$$\varphi_{02}(x)=\exp\left(-\frac{x^2}{2}\right)\left[2A_2\exp\left(-\frac{a_2^2}{2}\right)-B_2+A_2a_2^2x^2\times\exp\left(-\frac{a_2^2}{2}\right)+\frac{1}{12}A_2a_2^4x^4\exp\left(-\frac{a_2^2}{2}\right)+\cdots\right]. \tag{33}$$

If the conditions $|a_2x|<1$, $2A_2\exp(-a_2^2/2)-B_2=-2$, and $A_2a_2^2\exp(-a_2^2/2)=4$ are satisfied, Eq. (33) approaches Eq. (32) step by step with the decrease of the parameter $|a_2x|$.

The linear superposition of two in-phase and two out-of-phase Gaussian functions is

$$\varphi_{03}(x)=A_3\left\{\exp\left[-\frac{(x-2a_3)^2}{2}\right]-\exp\left[-\frac{(x+2a_3)^2}{2}\right]\right\}+B_3\left\{\exp\left[-\frac{(x+a_3)^2}{2}\right]-\exp\left[-\frac{(x-a_3)^2}{2}\right]\right\}=A_3\exp\left(-\frac{x^2+4a_3^2}{2}\right)[\exp(2a_3x)-\exp(-2a_3x)]-B_3\exp\left(-\frac{x^2+a_3^2}{2}\right)[\exp(a_3x)-\exp(-a_3x)]. \tag{34}$$

The third-order HG function can be written as

$$\varphi_3(x)=(8x^3-12x)\exp(-x^2/2). \tag{35}$$

Taylor expanding $[\exp(2a_3x)-\exp(-2a_3x)]$ and $[\exp(a_3x)-\exp(-a_3x)]$ with respect to x' at $x'=0$ in Eq. (34), one can obtain

$$\varphi_{03}(x)=\exp\left(-\frac{x^2}{2}\right)\left\{\left[4a_3A_3\exp(-2a_3^2)-2a_3B_3\times\exp\left(-\frac{a_3^2}{2}\right)\right]x+\left[\frac{8}{3}a_3^3A_3\exp(-2a_3^2)-\frac{B_3}{3}a_3^3\exp\left(-\frac{a_3^2}{2}\right)\right]x^3+\cdots\right\}. \tag{36}$$

If the conditions $|a_3x|<1$, $4a_3A_3\exp(-2a_3^2)-2a_3B_3\times\exp(-a_3^2/2)=-12$, and $(8/3)a_3^3A_3\exp(-2a_3^2)-(B_3/3)a_3^3\times\exp(-a_3^2/2)=8$ are satisfied, Eq. (36) approaches Eq. (35) step by step with the decrease of the parameter $|a_3x|$.

According to the same procedure introduced above, any higher-order HG function can be expressed by a linear superposition of Gaussian functions, out-of-phase between adjacent functions, under appropriate conditions. The potential application of the linear superposition method of the functions is to provide a new means to obtain the higher-order HG solitons experimentally.

The physical origin of the formation of such bound states follows naturally from the strongly nonlocal character of the nonlinear interaction. In SNNM, the nonlinear polarization of the medium with a small volume of radius x_0 (x_0 much less than any wavelength involved) is determined by the electric field distribution both inside the volume and outside the volume under consideration, the refractive index depends on the whole intensity distribution in the transverse plane, and the strongly nonlocality can lead to an increase of refractive index in the overlap region between out-of-phase solitons under the appropriate conditions. This creates an attractive force and leads to the formation of stable bound states consisting of a number of individual Gaussian solitons with a π phase difference between adjacent solitons if the initial amplitude of the individual solitons and the initial center distance between the individual solitons are chosen properly.

Figure 4 shows the comparisons of the first-, the second-, and the third-order-mode HG solitons and the stable bound states consisting of two out-of-phase Gaussian solitons, two in-phase and one out-of-phase Gaussian solitons, and two in-phase and two out-of-phase Gaussian solitons. It is easy from Fig. 4 to see that the HG solitons are in good agreement with the stable bound states consisting of several Gaussian solitons.

4. EXTENSION OF THE (1+1)-DIMENSIONAL CASE TO THE (1+2)-DIMENSIONAL CASE

In this section, the solutions from the (1+1)-dimensional case are extended to the (1+2)-dimensional case.

For the (1+2)-dimensional case, Eq. (2) in the Cartesian coordinate system can be rewritten as

$$i\frac{\partial\varphi^{(2)}}{\partial z}+\mu\left(\frac{\partial^2\varphi^{(2)}}{\partial x^2}+\frac{\partial^2\varphi^{(2)}}{\partial y^2}\right)-\frac{1}{2}k\eta\gamma P_0(x^2+y^2)\varphi^{(2)}=0. \tag{37}$$

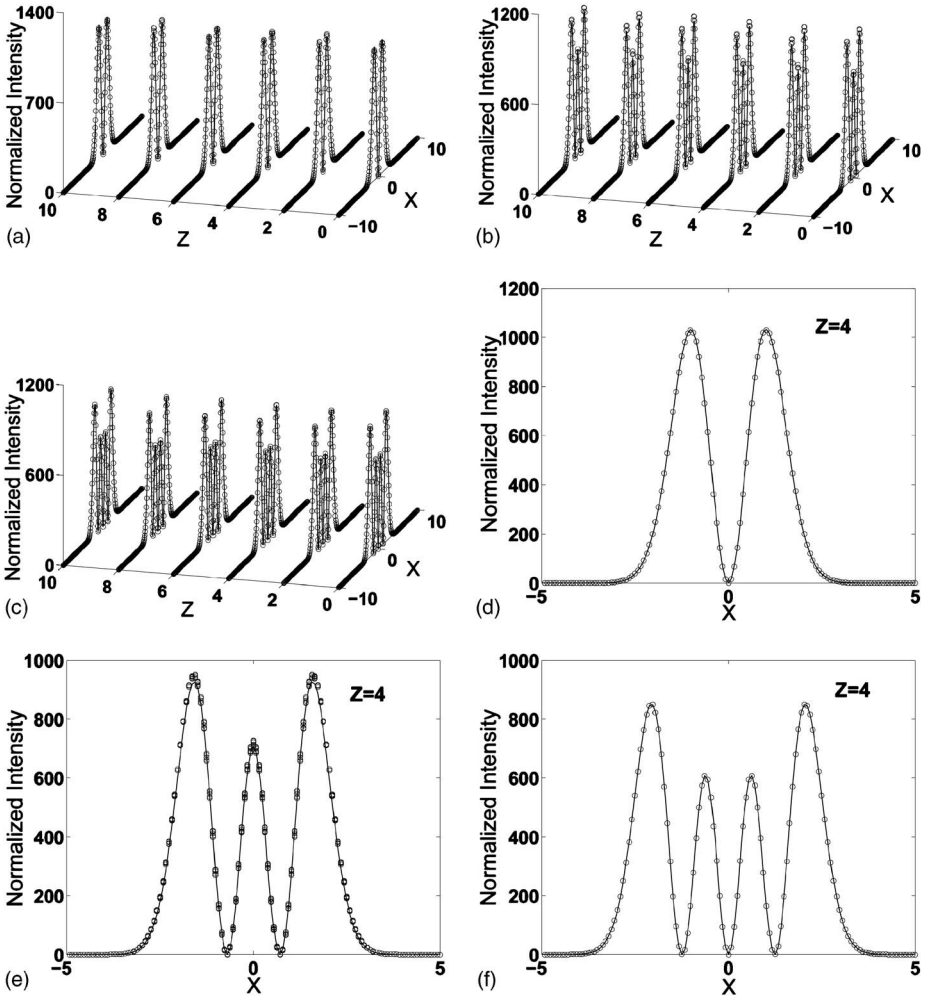

Fig. 4. Stationary propagation of the HG solitons (solid curves) and copropopagation of several Gaussian solitons (open circles) for (a) the first-order-mode HG soliton and two out-of-phase Gaussian solitons; (b) the second-order-mode HG soliton, two in-phase Gaussian solitons, and one out-of-phase Gaussian soliton; (c) the third-order-mode HG solitons and two in-phase and two out-of-phase Gaussian solitons in the Gaussian-shaped response material up to a distance of $Z=10$. Solid curves and open circles in (d), (e), and (f) are the normalized intensity distributions at $Z=4$ corresponding to (a), (b), and (c), respectively. The parameters are chosen as $P_0/P_c=1$, $\alpha=0.1$, $A_1=2.65$, $a_1=0.41$; $A_2=77.64$, $a_2=0.23$, $B_2=153.23$; $A_3=4091.01$, $a_3=0.1$, $B_3=8120.5$.

Following the same procedure as in Subsection 2.A, the exact solution of Eq. (37) can be obtained:

$$\varphi^{(2)}(x,y,z)=C_{mn}\frac{1}{w(z)}H_m\left(\frac{x}{w(z)}\right)H_n\left(\frac{y}{w(z)}\right)\exp\left[-\frac{(x^2+y^2)}{2w(z)^2}\right]\times\exp[ic(z)(x^2+y^2)]\times\exp[i2(m+n+1)\theta(z)], \tag{38}$$

where $C_{mn}=[P_0/(2^{m+n}\pi m!n!)]^{1/2}$ is the normalized coefficient, which can be obtained from $\int_{-\infty}^{\infty}\int_{-\infty}^{\infty}|\varphi^{(2)}\times(x,y,0)|^2dxdy=P_0$; $w(z)$, $c(z)$, $\theta(z)$, and P_c are given by Eqs. (9)–(12).

When $m=0$ and $n=0$, Eq. (38) is reduced to the zeroth-order HG (Gaussian) solution

$$\varphi_{00}=\frac{\sqrt{P_0}}{\sqrt{\pi}w(z)}\exp\left[-\frac{(x^2+y^2)}{2w(z)^2}\right]\exp[ic(z)(x^2+y^2)]\exp[i2\theta(z)]. \tag{39}$$

Equation (39) is the Gaussian solution obtained by Snyder and Mitchell [1] for the (1+2)-dimensional case. Equations (21) and (39) show that the solutions obtained by Snyder and Mitchell [1] are our lowest-order solutions for the (1+1)-dimensional and the (1+2)-dimensional cases, respectively.

5. CONCLUSION

Starting from the Snyder–Mitchell model in the Cartesian coordinate system, exact analytical HG solutions are derived in SNNM by using the method of separation of variables. The evolution of the HG beams in SNNM is discussed. The comparisons of analytical solutions with numerical simulations of the NNLSE show that the analyti-

cal HG solutions are in good agreement with the numerical results in the case of strong nonlocality. Our results show that the propagation constant increases as the mode number increases. We find that any higher-order HG function can be expressed in terms of the linear superposition of Gaussian functions with a π phase difference under the appropriate conditions. The Gaussian breather and the Gaussian soliton obtained by Snyder and Mitchell can be treated as special cases of the HG breathers and the HG solitons.

ACKNOWLEDGMENTS

This research was supported by the National Natural Science Foundation of China (grants 10474023 and 10674050) and Specialized Research Fund for the Doctoral Program of Higher Education (grant 20060574006).

REFERENCES

1. A. W. Snyder and D. J. Mitchell, "Accessible solitons," Science **276**, 1538–1541 (1997).
2. M. Peccianti, C. Conti, G. Assanto, A. D. Luca, and C. Umeton, "All-optical switching and logic gating with spatial solitons in liquid crystals," Appl. Phys. Lett. **81**, 3335–3337 (2002).
3. G. Assanto, M. Peccianti, and C. Conti, "Nematicons: optical spatial solitons in nematic liquid crystals," Opt. Photonics News **14**, 44–48 (2003).
4. D. J. Mitchell and A. W. Snyder, "Soliton dynamics in a nonlocal medium," J. Opt. Soc. Am. B **16**, 236–239 (1999).
5. W. Krolikowski, O. Bang, J. J. Rasmussen, and J. Wyller, "Modulational instability in nonlocal nonlinear Kerr media," Phys. Rev. E **64**, 016612 (2001).
6. C. Conti, M. Peccianti, and G. Assanto, "Route to nonlocality and observation of accessible solitons," Phys. Rev. Lett. **91**, 073901 (2003).
7. C. Conti, M. Peccianti, and G. Assanto, "Observation of optical spatial solitons in a highly nonlocal medium," Phys. Rev. Lett. **92**, 113902 (2004).
8. Q. Guo, B. Luo, F. Yi, S. Chi, and Y. Xie, "Large phase shift of nonlocal optical spatial solitons," Phys. Rev. E **69**, 016602 (2004).
9. Q. Guo, "Nonlocal spatial solitons and their interactions," in *Optical Transmission, Switching, and Subsystems*, C. F. Lam, C. Fan, N. Hanik, and K. Oguchi, eds., Proc. SPIE **5281**, 581–594 (2004).
10. Y. Xie and Q. Guo, "Phase modulations due to collisions of beam pairs in nonlocal nonlinear media," Opt. Quantum Electron. **36**, 1335–1351 (2004).
11. A. V. Mamaev, A. A. Zozulya, V. K. Mezentsev, D. Z. Anderson, and M. Saffman, "Bound dipole solitary solutions in anisotropic nonlocal self-focusing media," Phys. Rev. A **56**, R1110–R1113 (1997).
12. M. Peccianti, K. A. Brzdakiewicz, and G. Assanto, "Nonlocal spatial soliton interactions in nematic liquid crystals," Opt. Lett. **27**, 1460–1462 (2002).
13. X. Hutsebaut, C. Cambournac, M. Haelterman, A. Adamski, and K. Neyts, "Single-component higher-order mode solitons in liquid crystals," Opt. Commun. **233**, 211–217 (2004).
14. Z. Xu, Y. V. Kartashov, and L. Torner, "Upper threshold for stability of multipole-mode solitons in nonlocal nonlinear media," Opt. Lett. **30**, 3171–3173 (2005).
15. S. Skupin, O. Bang, D. Edmundson, and W. Krolikowski, "Stability of two-dimensional spatial solitons in nonlocal nonlinear media," Phys. Rev. E **73**, 066603 (2006).
16. A. I. Yakimenko, V. M. Lashkin, and O. O. Prikhodko, "Dynamics of two-dimensional coherent structures in nonlocal nonlinear media," Phys. Rev. E **73**, 066605 (2006).
17. N. I. Nikolov, D. Neshev, W. Krolikowski, O. Bang, J. J. Rasmussen, and P. L. Christiansen, "Attraction of nonlocal dark optical solitons," Opt. Lett. **29**, 286–288 (2004).
18. A. Dreischuh, D. Neshev, D. E. Petersen, O. Bang, and W. Krolikowski, "Observation of attraction between dark solitons," Phys. Rev. Lett. **96**, 043901 (2006).
19. D. W. McLaughlin, D. J. Muraki, M. J. Shelley, "Self-focussed optical structures in a nematic liquid crystal," Physica D **97**, 471–497 (1996).
20. C. Rotschild, M. Segev, Z. Y. Xu, Y. V. Kartashov, L. Torner, and O. Cohen, "Two-dimensional multipole solitons in nonlocal nonlinear media," Opt. Lett. **31**, 3312–3314 (2006).
21. D. Buccoliero, A. S. Desyatnikov, W. Krolikowski, and Y. S. Kivshar, "Laguerre and Hermite soliton clusters in nonlocal nonlinear media," Phys. Rev. Lett. **98**, 053901 (2007).
22. A. W. Snyder and Y. Kivshar, "Bright spatial solitons in non-Kerr media: stationary beams and dynamical evolution," J. Opt. Soc. Am. B **11**, 3025–3031 (1997).
23. S. Abe and A. Ogura, "Solitary waves and their critical behavior in a nonlinear nonlocal medium with power-law response," Phys. Rev. E **57**, 6066–6070 (1998).
24. B. Granot, S. Sternklar, Y. Isbi, B. Malomed, and A. Lewis, "Sub-wavelength non-local spatial solitons," Opt. Commun. **166**, 121–126 (1999).
25. W. Krolikowski and O. Bang, "Solitons in nonlocal nonlinear media: exact solutions," Phys. Rev. E **63**, 016610 (2000).
26. S. G. Ouyang, Q. Guo, and W. Hu, "Perturbative analysis of generally nonlocal spatial optical solitons," Phys. Rev. E **74**, 036622 (2006).
27. P. D. Rasmusen, O. Bang, W. Królikowski, "Theory of nonlocal soliton interaction in nematic liquid crystals," Phys. Rev. E **72**, 066611 (2005).
28. X. P. Zhang and Q. Guo, "Analytical solution in the Hermite–Gaussian form of the beam propagating in the strong nonlocal media," Acta Phys. Sin. **54**, 3178–3182 (2005) (in Chinese).
29. X. P. Zhang and Q. Guo, "Analytical solution to the spatial optical solitons propagating in the strong nonlocal media," Acta Phys. Sin. **54**, 5189–5193 (2005) (in Chinese).
30. W. Hu, T. Zhang, Q. Guo, L. Xuan, and S. Lan, "Nonlocality-controlled interaction of spatial solitons in nematic liquid crystals," Appl. Phys. Lett. **89**, 071111 (2006).
31. Y. R. Shen, "Optical physics—solitons made simple," Science **276**, 1520–1520 (1997).
32. W. Krolikowski, M. Saffman, B. Luther-Davies, and C. Denz, "Anomalous interaction of spatial solitons in photorefractive media," Phys. Rev. Lett. **80**, 3240–3243 (1998).
33. G. E. Andrews, R. Askey, and R. Roy, *Special Functions* (Cambridge U. Press, 2000), Sec. 6.1.